Available online at www.sciencedirect.com
SCIENCE DIRECT®
Journal of Sound and Vibration 268 (2003) 485–501
JOURNAL OF SOUND AND VIBRATION
www.elsevier.com/locate/jsvi

Dynamic studies of railtrack sleepers in a track structure system

G. Kumaran, Devdas Menon*, K. Krishnan Nair

Department of Civil Engineering, Indian Institute of Technology, Chennai 600 036, India

Received 31 May 2002; accepted 20 November 2002

Abstract

This paper discusses the dynamic response of a typical prestressed concrete railtrack sleeper due to wheel–track interaction dynamics, involving wheel and rail imperfections, under various parametric conditions. The interaction dynamics of the vehicle and track is first carried out in the time domain using MSC/NASTRAN. Using the resulting load time histories on an isolated sleeper, a detailed finite element model of the sleeper is used to analyze its dynamic behaviour. The dynamic amplification factors for deflection, ballast pressure and bending moments have been evaluated at the critical section (rail-seat and centre) for various exciting frequencies under different vehicle–track parametric conditions. The results provide a basis for improved and rational design of the sleeper.

1. Introduction

The prestressed concrete monoblock sleeper is well recognized as a vital constituent of the modern railway track structure. Such sleepers were first introduced in 1943 at Cheddington in the UK on an experimental basis [1–3]. The primary function of the railtrack sleeper is to transmit the wheel load to the ballast medium. In addition to the above, it has additional functions such as maintaining track alignment and gauge, restraining longitudinal and lateral rail movements, and providing strength and stability to track structure. The superiority of the prestressed concrete sleeper, in comparison with other sleepers made of timber, steel, cast iron or reinforced concrete, lies in its improved structural performance, in terms of stability,

*Corresponding author.
E-mail addresses: ganapathykumaran@rediffmail.com (G. Kumaran), dmenon@civil.iitm.ernet.in (D. Menon), kknair@lycos.com (K. Krishnan Nair).

0022-460X/03/$ - see front matter
doi:10.1016/S0022-460X(02)01581-X

stiffness, strength, improved resistance to fatigue loading and durability [4]. Other major factors include convenience in mass production with high-quality control and relative economy (involving least life cycle cost).

The present-day design of railtrack sleepers is largely based on simplified analysis using prescribed equivalent loading and uniformly varying ballast pressure distribution. Generally, the pressure distribution is assumed to be uniform (p) under the rail-seat portions, and in the central region, is taken as αp, where α is termed the 'centre binding coefficient', having a value less than unity.

These simplified design bases, however, do not account explicitly for the influence of the elastic properties of sleeper, ballast and subgrade, and the possible effects of non-uniform contact at the sleeper–ballast interface. The prescribed simplified methods of railtrack sleeper design continue to be based on approximate load modelling and analysis. Such analytical procedures have been prescribed by the American Railway Engineering Manual (AREMA) and the Research Design Standards Organisation (RDSO), Indian Railways [1,5].

Although considerable research has been done in the area of vehicle–rail interaction in the past, analysis of the dynamic response of the sleeper in isolation is a problem that has not received sufficient attention. The dynamic nature of the loading is not only due to the wheel–track interaction, but also due to wheel and rail imperfections [6–10].

Analytical studies by the authors have shown that the ballast pressure distributions obtained from both static and dynamic analyses are highly non-uniform and the critical sections are obtained at the rail-seat and at the centre of the sleeper [11]. The aim of the present work is to assess the prevailing analytical procedures of railtrack sleepers on the basis of more rigorous modelling and analysis, and to make improved recommendations for more rational design.

In order to examine the behaviour of sleepers in a railtrack structure, a model involving all components of the track structure and vehicle parameters is required. In this paper, the response of the railtrack sleeper is investigated in a track structure system, considering the vehicle (axle type), condition of the suspension system, vehicle speed, contact between wheel and rail, wheel and rail defects (irregularities), as well as non-uniform contact between sleeper and ballast.

Three models are considered for the dynamic analysis of the railtrack sleeper in the track structure system, viz., 'vehicle' model, 'track' model and 'sleeper in isolation' model. The vehicle and track models are used to determine the rail-seat load history that is transmitted to the sleepers during the passage of the vehicle, considering different imperfections such as rail corrugations, wheel-flats and rail joints. In the track model, a track length encompassing 12 sleepers is considered. The interaction between the vehicle and track is carried out in the time domain using the finite element software MSC/NASTRAN. The results from the track structure model are then used as load time histories on an isolated sleeper model that focuses on the detailed studies of its dynamic behaviour, in terms of deflection, ballast pressure and bending moment responses. The results depict the nature of the non-uniform distribution of ballast pressures and dynamic amplification factors under different exciting frequencies. The stress resultants (peak bending moments) are obtained from the rigorous dynamic analysis. The results obtained are used to formulate an equivalent static model to facilitate practical design of railtrack sleepers. This provides a rational basis for improved design recommendations.

2. Rigorous modelling of vehicle and track structure

2.1. Modelling of vehicle

Fig. 1 illustrates the train vehicle model adopted in this study conforming to Indian railways. It consists of a vehicle body, two bogie frames and four wheel sets. The vehicle is modelled as a rigid body having a mass m_c, and having second moments of area J_{cx} and J_{cy} about the transverse and longitudinal centroidal horizontal axes, respectively. Similarly, each bogie frame is considered as a rigid body with a mass m_b (m_{b1} and m_{b2}) with second moments of area J_{bx} and J_{by} about the transverse and longitudinal centroidal horizontal axes, respectively. Each axle along with the wheel set has a mass m_w (for four axles m_{w1}, m_{w2}, m_{w3}, and m_{w4}). The spring and the shock absorber in the primary suspension for each axle are characterized by spring stiffness k_p and damping coefficient c_p, respectively. Likewise, the secondary suspension is characterized by spring stiffness k_s and damping coefficient c_s, respectively.

The various displacements of the vehicle are described with respect to the equilibrium positions. As the vehicle car body is assumed to be rigid, its motion may be described by the vertical displacement (bounce or z_c) and rotations about the transverse horizontal axis (pitch or θ_c) and about the longitudinal horizontal axis (roll or ϕ_c). Similarly, the movements of the two bogie units are described by three degrees of freedom z_{b1}, θ_{b1} and ϕ_{b1} each about their centriods. Each axle set is described by two degrees of freedom z_{w1}, and ϕ_{w1} about their centriods. Totally, 17 degrees of freedom have been considered in this study for the vehicle model shown in Fig. 1 [12–14]. The displacement vector $\{y_t\}$ for the train vehicle can therefore be written in terms of displacements at the centriod of the vehicle body z_c, θ_c and ϕ_c, the displacements at the centriods of the bogie

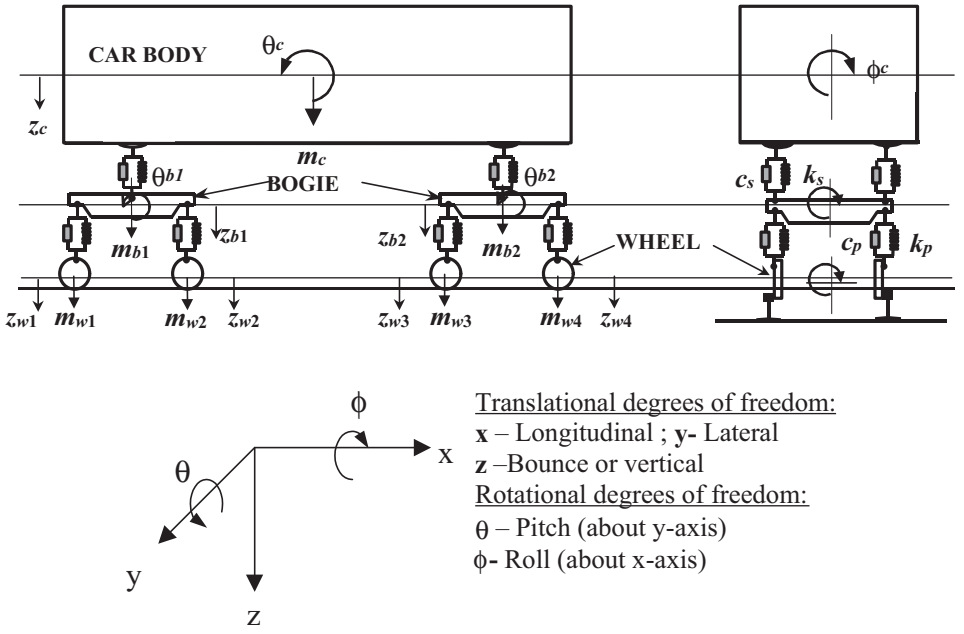

Fig. 1. Model of Railway Vehicle.

frames z_{b1}, θ_{b1}, ϕ_{b1}, z_{b2}, θ_{b2} and ϕ_{b2}, and the displacements of the four axles z_{w1}, ϕ_{w1}, z_{w2}, ϕ_{w2}, z_{w3}, ϕ_{w3}, z_{w4}, and ϕ_{w4} as

$$\{y_t\} = \left\{ \begin{matrix} z_c, z_{b1}, z_{b2}, z_{w1}, z_{w2}, z_{w3}, z_{w4}, \theta_c, \theta_{b1}, \\ \theta_{b2}, \phi_c, \phi_{b1}, \phi_{b2}, \phi_{w1}, \phi_{w2}, \phi_{w3}, \phi_{w4} \end{matrix} \right\}. \tag{1}$$

The reactions at the left and right points on the rails are expressed in terms of the static reactive components W_L and W_R, respectively, and are given as

$$W_L \quad \text{or} \quad W_R = \frac{m_c g}{4} + \frac{m_b g}{2} + m_w g. \tag{2}$$

Similarly, the dynamic reactions at the left and right points on the rails are expressed in terms of the dynamic reactive components $W_L(t)$ and $W_R(t)$, respectively. Non-linearities in the behaviour of the both primary and secondary suspension units are not considered in the present study.

The response is obtained when the vehicle traverses 12 sleeper bays of a model of a railway track with the constant speed. An initially straight track with imperfections and without imperfections is considered. The vertical dynamic response of railtrack sleeper excited under moving multi-axle loads on track structure is investigated. The wheels of the train are assumed to have infinite stiffness. It is also assumed that there is no loss of contact between the wheels of the vehicle and the rails. A Digital Power FORTRAN subroutine has been written to perform dynamic analysis of the vehicle effectively using direct integration technique. The equation of motion for the vehicle model consisting of carbody, bogie units and wheel sets are derived from rigid-body idealization, and can be expressed as

$$\mathbf{m}\ddot{\mathbf{y}} + \mathbf{c}\dot{\mathbf{y}} + \mathbf{k}\mathbf{y} = \mathbf{W}(t), \tag{3}$$

where $\mathbf{m}$, $\mathbf{c}$ and $\mathbf{k}$ are the mass, damping and stiffness matrices of the vehicle, respectively, and $\mathbf{W}(t)$ is the load vector.

2.2. Modelling of track structure

In the present study, a linear 3-D finite element model (Fig. 2) of the railway track structure is considered, accounting for the elastic properties of rail-pad, ballast, different ballast contact between sleeper and ballast along the sleeper length, sub-ballast and sub-soil stiffness. The rail section is modelled as solid elements, resting on discrete supports of rail-pad. The rail-pad is

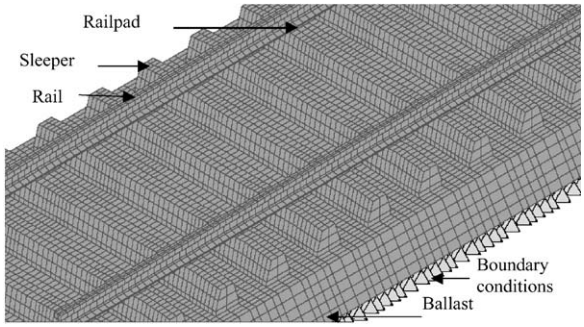

Fig. 2. Finite element model of track structure.

modelled as a spring element, which has vertical stiffness k_{pad} and viscous damping c_{pad}. The spring behaviour of the rail fastenings with an uplift motion of the rail is not considered in this study. The sleeper, ballast and sub-ballast are modelled as three-dimensional solid elements, accounting for their elastic properties. The contact between the sleeper and the ballast is considered along the sleeper length. The substrata are modelled using linear boundary elements and absorbing boundary conditions. In this study, the absorbing or silent boundary conditions are imposed at the base of the horizontal ballast of the finite model. The finite boundaries of such model of the soil medium should be such that the elastic waves, which propagate through the medium, do not reflect back from these boundaries to the vibrating medium [15–19]. The length of the track considered is limited to 12 sleeper bays, primarily in view of the excessive computational time required to solve the 3-D dynamic interaction problem through numerical integration in the time domain. However, the results of the dynamic analysis show that the track length adopted is sufficient to capture the peak response due to the passage of a full train of 12 bogie units at constant speed.

3. Dynamic analysis of railtrack sleepers in track structure

3.1. Track inputs to railway vehicles

The dynamic wheel loads generated by a moving train are mainly due to various wheel/track imperfections. These imperfections are considered as the primary source of dynamic track input to the railroad vehicles. Normally, the imperfections that exist in the railtrack structure are associated with the vertical track profile, cross level, rail joint, wheel flatness, wheel/rail surface corrugations and uneven support of the sleepers.

For the present study, the average vertical profile data on left and right rails of a continuously welded mainline track of the Indian railway are used. These data are obtained from the Indian Railways Research Design and Standards Organisation, Lucknow, based on actual rail track measurements [21]. The average vertical profile data of a continuously welded mainline track of the Indian railway have been superimposed on the periodic irregularities (repeated rail joint along with wheel flatness) to provide realistic track input to the vehicle model. The initial excitation forces due to the track irregularities applied to the vehicle model are $F(t) = k_p y(t)$, where $y(t)$ is the average vertical profile of the track. The initial excitation force due to the track irregularities are fed to the vehicle system at each primary suspension unit of wheels with time lags of $t(l/v)$ corresponding to the distances between two consecutive axles l. These force inputs are repeated between successive time intervals till the complete length of train passes out with constant velocity v.

3.2. Interaction analysis

The dynamic interaction of combined systems such as vehicle and track needs special attention when the fast moving heavy vehicles interact with the track structure. The objective of the interaction analysis is to determine the time histories of the wheel load reactions transmitted to the

sleeper. These can be expressed as follows (detailed derivation is given in Appendix A):

$$W_L(t) = m_w\ddot{z}_{w1} + 2c_p\dot{z}_{w1} - 2c_p\dot{z}_{b1} + 2c_p l_b\dot{\theta}_{b1} + 2k_p z_{w1} - 2k_p z_{b1} + 2k_p l_b\theta_{b1} + 2k_w z_{w1} - J_{wx}\ddot{\phi}_{w1} + 2c_p l_g\dot{\phi}_{w1}l_p + 2c_p l_b\dot{\phi}_{b1}l_p - 2k_w\phi_{w1}l_g^2 + 2k_p l_g\phi_{w1}l_p + 2k_p l_b\phi_{b1}l_p, \quad (6)$$

$$W_R(t) = m_w\ddot{z}_{w1} + 2c_p\dot{z}_{w1} - 2c_p\dot{z}_{b1} + 2c_p l_b\dot{\theta}_{b1} + 2k_p z_{w1} - 2k_p z_{b1} + 2k_p l_b\theta_{b1} + 2k_w z_{w1} + J_{wx}\ddot{\phi}_{w1} - 2c_p l_g\dot{\phi}_{w1}l_p - 2c_p l_b\dot{\phi}_{b1}l_p + 2k_w\phi_{w1}l_g^2 - 2k_p l_g\phi_{w1}l_p - 2k_p l_b\phi_{b1}l_p, \quad (7)$$

where $W_L(t)$ and $W_R(t)$ are the reactions at the left and right rail, respectively. The equation of motion for the entire vehicle track structure is written as

$$\begin{bmatrix} \mathbf{m}_V & 0 \\ 0 & \mathbf{m}_T \end{bmatrix}\ddot{\mathbf{y}} + \begin{bmatrix} \mathbf{c}_V & 0 \\ 0 & \mathbf{c}_T \end{bmatrix}\dot{\mathbf{y}} + \begin{bmatrix} \mathbf{k}_V & 0 \\ 0 & \mathbf{k}_T \end{bmatrix}\mathbf{y} = \mathbf{W}(t), \quad (8)$$

where $\mathbf{m}_V$, $\mathbf{c}_V$ and $\mathbf{k}_V$ are the mass, damping and stiffness matrices of the vehicle system, respectively, and the corresponding parameters with the subscript T refers to the track system. The external force vector $\mathbf{W}(t)$ resulting from the wheel loads is dependent on the wheel and track (rail) interaction, and hence is time dependent.

The interaction between vehicle and track is solved numerically in time-domain approach. In this study, a digital visual FORTRAN code is written to calculate the vertical response of the vehicle by direct integration technique using Newmark β method. The free vibration analysis is carried for the combined vehicle and track system using MSC/NASTRAN software. The time steps for direct integration are calculated from the natural frequency of the combined vehicle and track system. The minimum time step to carry out the direct integration scheme is taken as one-tenth of the fundamental time period, in the interest of numerical stability [20,21]. The dynamic wheel reaction from the vehicle model is fed to the 3-D finite element track model. The compatibility conditions are satisfied at each node and at each time step by considering the displacements of wheel and the displacement of rail. Fig. 4 illustrates vehicle–track interaction analysis in time domain.

3.3. Dynamic load on railtrack sleeper

The reaction force (P_t) at the rail seat portion of the sleeper in the sleeper model is calculated as the sum of the reaction forces obtained in the nodes of the finite element model, where the displacement history is obtained [22,23]. The dynamic load history near the rail seat location, $P(t)$ is obtained as

$$P(t) = k_{pad}(z_s - z_r) + c_{pad}(\dot{z}_s - \dot{z}_r), \quad (9)$$

where k_{pad} and c_{pad} are the rail-pad stiffness and damping, respectively; z_r and z_s are the vertical displacements of the rail and the sleeper at the rail-seat locations, respectively, and $\dot{z}_r$ and $\dot{z}_s$ are the vertical velocities of the rail and the sleeper, respectively.

3.4. Dynamic analysis of sleeper in isolation

A railtrack sleeper unit separated from track structure is modelled in finite element analysis software (MSC/NASTRAN) to obtain the detailed dynamic response of the individual sleeper.

This model consists of one sleeper unit, supported on ballast, sub-ballast and sub-strata, and is modelled using solid elements. The substrata are modelled as boundary elements with absorbing boundaries. A detailed dynamic analysis is carried using the rail-seat load history as an input to the sleeper in isolation model. The detailed dynamic response quantities of interest are the deflection, ballast pressure and bending moment and their dynamic amplification factors (ψ). The ballast pressures are generated from the nodal forces at the sleeper–ballast interface (output of finite element analysis), and the bending moments are obtained from these, based on the static equilibrium of the sleeper in isolation. The responses are plotted for different exciting frequencies and different parametric conditions at the two critical section, viz., centre and rail-seat.

The computational feasibility of the track model depends on the meshing criteria adopted. A very fine meshing of the track model is not computationally feasible as it requires enormous computing capacity. Moreover, the global response of railtrack sleepers in railtrack system is not much sensitive to the criteria adopted. Hence in this study, a finer finite element meshing criteria is adopted only for the sleeper in isolation model to achieve improved accuracy.

4. Results and parametric study

A parametric study is carried out for different vehicle and track parameters that influence the dynamic behaviour of railtrack sleepers in the track structure. The factors considered for parametric study are given below.

Vehicle parameters: Mass of car body $m_c = 70\,000$ kg; mass of bogie unit $m_b = 5800$ kg; mass of wheel-set $m_w = 1900$ kg. Stiffness of primary suspension springs (per wheel) $k_p = 1260$ N/mm; vertical damping of primary suspension: $c_p = 20$ N s/mm; stiffness of secondary suspension springs $k_s = 900$ N/mm and vertical damping of secondary unit $c_p = 60$ N s/mm.

Track parameters: Mass per unit length (Rail UIC) = 60 kg/m; sleeper elastic modulus $E_c = 38\,450$ MPa; sleeper spacing = 600 mm; elastic modulus of ballast $E_b = 150$–350 MPa [16].

Rail-pad parameters: Rail-pad stiffness (k_{pad}) and damping (c_{pad}) of (a) soft pad: $k_{pad} = 100$ kN/mm and $c_{pad} = 43$ Ns/mm, (b) stiff pad: $k_{pad} = 600$ kN/mm and $c_{pad} = 93$ N s/mm [10]; the 'no rail-pad' condition (when the rail-pad gets dislodged and the rail is directly in contact with the sleeper) is also investigated separately.

Centre binding between the sleeper and ballast: Two extreme cases are considered: (i) total loss of contact in the central region (which occurs in the early life of the track structure) and (ii) full contact at all points (which occurs subsequently).

Elastic properties of subgrade: stiffness (k_{sub}) = 200–600 kN/mm; density of subgrade medium (ρ) = 18×10^{-6} N/mm^3; The Poissons' ratio (η) = 0.33 and shear wave velocity (V_s) = 150 m/s (which is well above the critical speed C_T of the train, in the order of 30–40 m/s, is adopted in most of the stretches in India) [5].

4.1. Dynamic loading on sleeper at rail-seat

Some typical results of the dynamic analysis are depicted in the form of graphs comprising load histories under different train speeds at the rail-seat locations (Figs. 3 and 4). The time lag between successive peaks is associated with the spacing of wheels. The dynamic load amplification

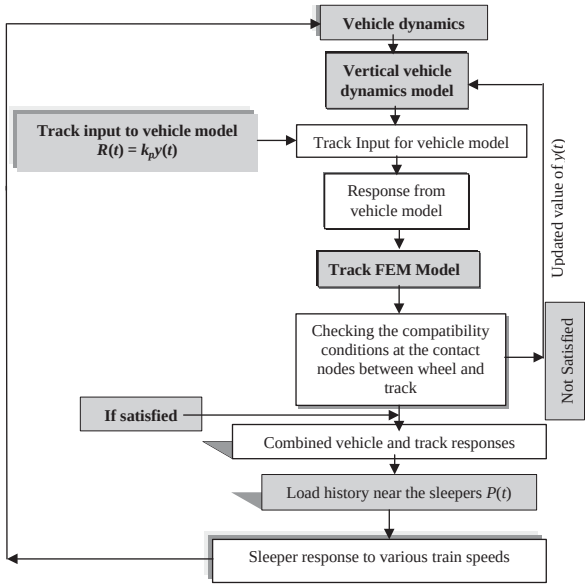

Fig. 3. Flow chart illustrating vehicle-track interaction analysis in time domain.

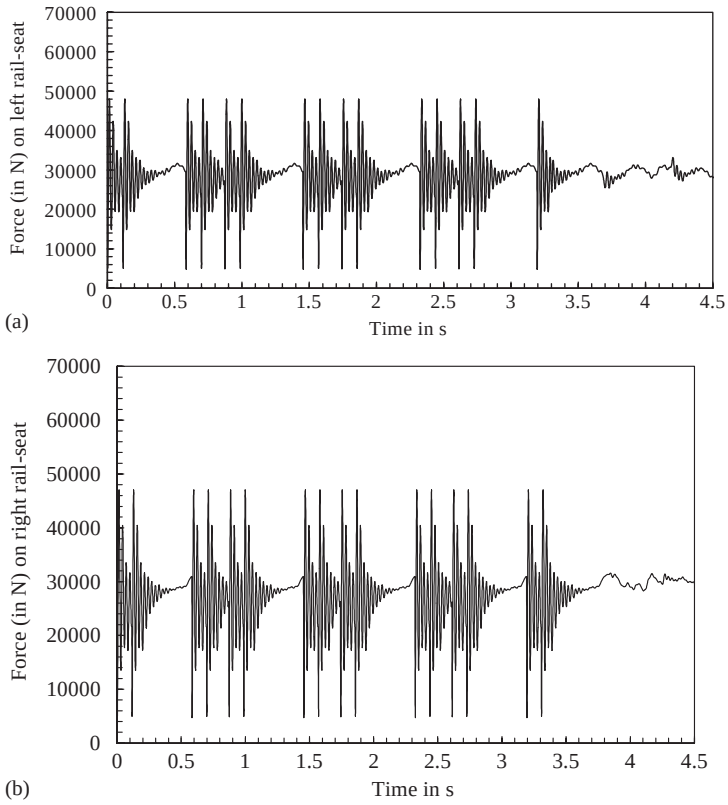

Fig. 4. Dynamic load history near the left and right rail-seat areas for $E_b = 350$ MPa, 'no rail-pad' condition and $k_{sub} = 600$ kN/mm.

factors (ψ_L) at the rail-seat locations for some typical parametric conditions are given in the form of graphs (Figs. 5–8). The inferences from these graphs are as follows:

- Peak values of ψ_L occur in the exciting frequencies frequency range of 100–250 Hz (i.e., vehicle speeds of 70–120 kmph).
- Values of ψ_L increase with increase in elastic modulus of ballast (E_b), decrease in rail-pad stiffness (k_{pad}), increase in subgrade stiffness (k_{sub}) and loss of contact at centre.
- Absolute maximum peak load amplification factor is found to be 2.55, corresponding to $E_b =$ 350 MPa, 'no rail-pad' condition, $k_{sub} = 600$ kN/mm and loss of contact at centre.
- Values of ψ_L are low and independent of exciting frequency when irregularities are absent in the wheel and rail, suggesting that these imperfections are mainly responsible for dynamic effects.

4.2. Dynamic response amplification factors in sleeper design

The dynamic load histories at rail-seat are given as input to the 'sleeper in isolation' model. From the dynamic analysis of the sleeper in isolation model, the peak dynamic response is obtained and by comparing with the values obtained from static analysis, amplification factors for

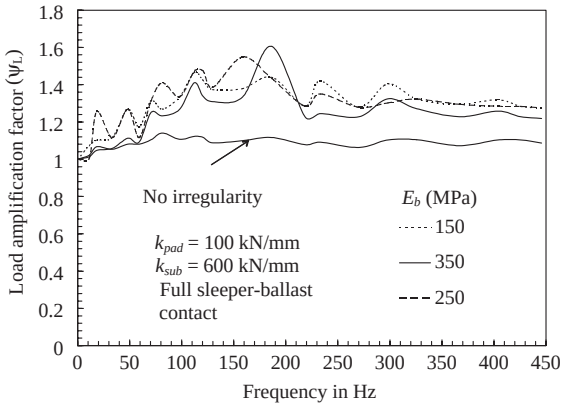

Fig. 5. Load amplification factors (ψ_L) vs frequency for 'no rail-pad' condition, $k_{sub} = 600$ kN/mm and Full contact.

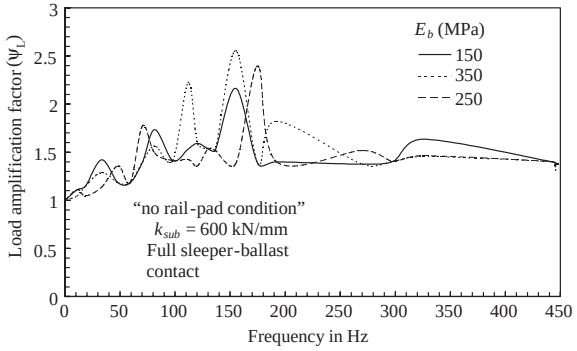

Fig. 6. Load amplification factors (ψ_L) vs frequency for 'no rail-pad' condition, $k_{sub} = 200$ kN/mm and Full contact.

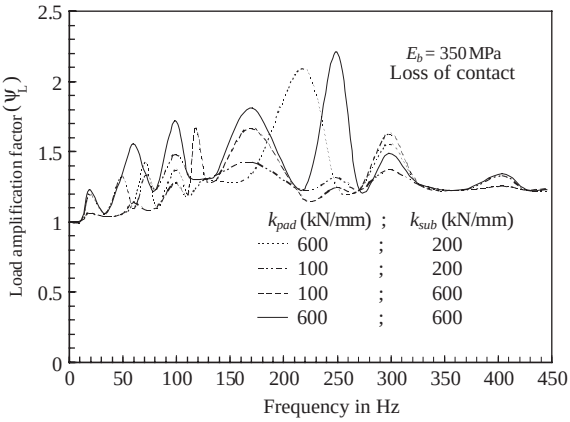

Fig. 7. Load amplification factors (ψ_L) vs frequency for $k_{pad} = 100$–$600\,\mathrm{kN/mm}$, $E_b = 350\,\mathrm{MPa}$ and Loss of contact.

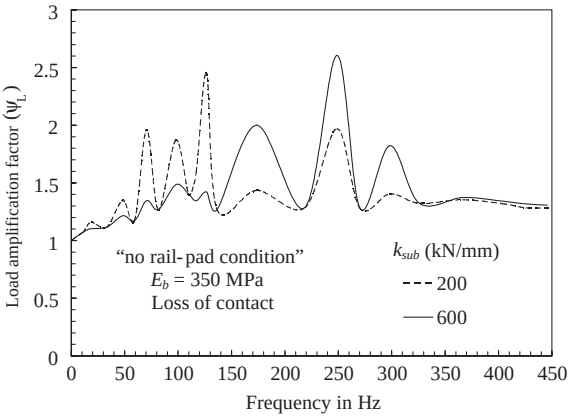

Fig. 8. Load amplification factors (ψ_L) vs frequency for 'no rail-pad' condition, $E_b = 350\,\mathrm{MPa}$ and Loss of contact.

bending moment ψ_M, ballast pressure ψ_B and deflection ψ_D are derived (Figs. 9–12). The numerical values of the static moment (M_{stat}), dynamic moment (M_{dyn}) and the corresponding values of the amplification factors ($\psi_M = M_{dyn}/M_{stat}$) for the critical parametric conditions are illustrated in Table 1.

The detailed static analysis results based on the parametric study are reported elsewhere [22]. In addition to the inferences drawn with respect to the dynamic load amplification factor ψ_L, the following conclusions are drawn based on the Figs. 9–12 and Table 1.

- It is observed that invariably $\psi_D > \psi_B > \psi_M$ at the critical locations of rail-seat and centre for any given exciting frequency. However, from a sleeper design point of view, it is the moment magnification factor ψ_M that is significant.
- The amplification factors for bending moment ψ_M, ballast pressure ψ_B and deflection ψ_D increase with increase in elastic modulus of ballast (E_b), decrease in rail-pad stiffness (k_{pad}),

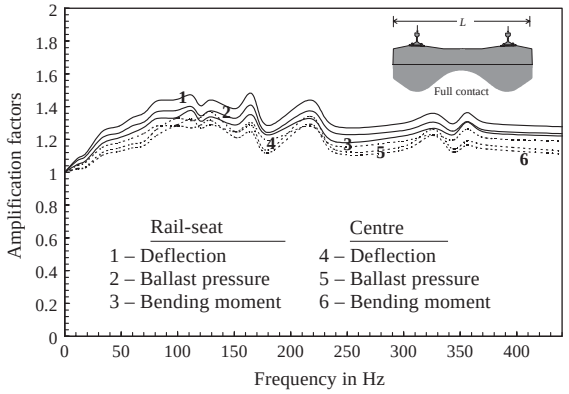

Fig. 9. Sleeper in isolation model: Amplification factors vs frequencies for $E_b = 150\,\text{MPa}$, $k_{pad} = 600\,\text{kN/mm}$, $k_{sub} = 200\,\text{kN/mm}$ and Full contact.

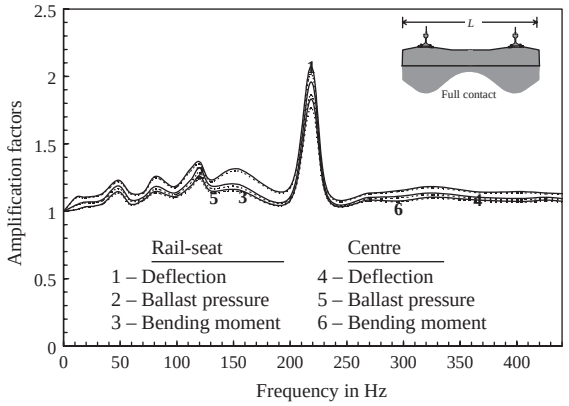

Fig. 10. Sleeper in isolation Model: Amplification factors vs frequencies for $E_b = 350\,\text{MPa}$, 'no rail-pad' condition, $k_{sub} = 600\,\text{kN/mm}$ and Full contact.

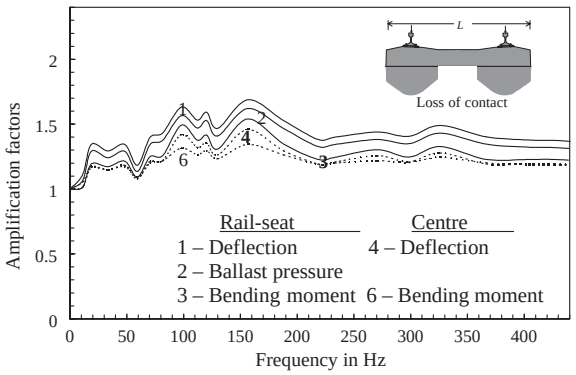

Fig. 11. Sleeper in isolation model: Amplification factors vs frequencies for $E_b = 350\,\text{MPa}$, $k_{pad} = 600\,\text{kN/mm}$, $k_{sub} = 200\,\text{kN/mm}$ and Loss of contact.

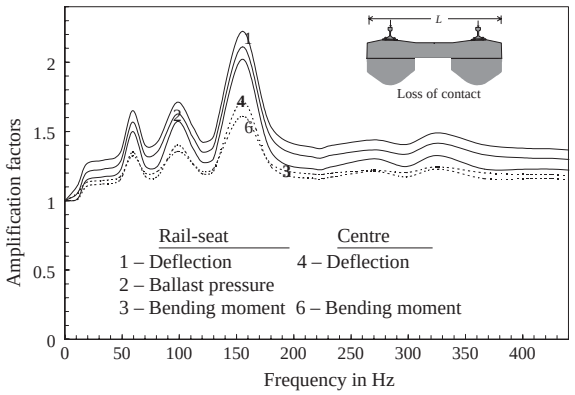

Fig. 12. Sleeper in isolation model: Amplification factors vs frequencies for $E_b = 350$ MPa, 'no rail-pad' condition, $k_{sub} = 600$ kN/mm and Loss of contact.

Table 1
Numerical results of parametric study

Condition	Fig. no.	Rail-seat			Centre		
		M_{stat} (kNm)	M_{dyn} (kNm)	$\psi_M = \frac{M_{dyn}}{M_{stat}}$	M_{stat} (kNm)	M_{dyn} (kNm)	$\psi_M = \frac{M_{dyn}}{M_{stat}}$
Full contact	9	3.13	4.41	1.41	3.38	4.50	1.33
	10	4.23	8.29	1.96	5.61	10.60	**1.89**
Loss of contact	11	4.12	6.72	1.63	2.36	3.10	1.31
	12	5.12	10.54	**2.06**	2.81	4.52	1.61

increase in subgrade stiffness (k_{sub}) and loss of contact at centre. These trends are similar to those observed in Figs. 5–8.

- A sharp peak in the dynamic response is observed under 'no rail-pad' condition. The corresponding exciting frequency is 215 Hz under full contact condition and 160 Hz under loss of contact (at centre) condition.
- Corresponding to $E_b = 350$ MPa, "no rail-pad" condition and $k_{sub} = 600$ kN/mm, absolute maximum peak moment amplification factor ψ_M are obtained: $\psi_M = 2.06$ at rail-seat (under loss of contact at centre) and $\psi_M = 1.89$ centre (corresponding to full contact).
- For the full contact condition, it is observed that the dynamic amplification factor ψ_M at the rail-seat is invariably higher as compared to the centre even though the dynamic bending moment is lower at the rail-seat as compared to the centre (Figs. 9 and 10, Table 1).
- It is also observed that when there is loss of contact between sleeper and ballast, the static and dynamic moments at rail-seat is relatively higher as compared to the centre of the sleeper (Figs. 11 and 12, Table 1).

5. Conclusions

A rigorous mathematical model, including the vehicle (with 17 degrees of freedom) and track structure is investigated, considering vehicle suspension system, speed, wheel and rail irregularities and elastic properties of the rail-pad and ballast–subgrade. The common imperfections, due to railjoints, wheel flatness and track unevenness, have been considered in the dynamic input to the vehicle model. The damping characteristics of the track and the railway vehicle have also been considered. The effect of the semi-infinite medium of subsoil is considered by imposing silent boundary conditions at the base of the horizontal ballast of the finite model. The elastic properties of the equivalent Winkler springs are derived based on the shear wave velocity of the medium. The dynamic interactive analysis is carried out between the vehicle and track in the time domain using MSC/NASTRAN finite element software. The results of the interactive analysis give responses in the form of reaction time histories at the rail-seat locations during the passage of vehicle. Comparison with the results of static finite element analysis yields values of dynamic load amplification factors under different vehicle–track parametric condition.

The rail-seat load histories obtained from the interactive model are fed into the sleeper in isolation 3-D model to obtain the detailed dynamic behaviour of the railtrack sleeper. A parametric study is carried out to assess the influence of different track parameters on the dynamic behaviour of the railtrack sleepers. The dynamic amplification factors for deflection, ballast pressure and bending moments have been evaluated at the critical sections (rail-seat and centre) for various exciting frequencies under different vehicle–track parametric conditions. The amplification factors for bending moment are of particular relevance in the design of the sleepers. It is observed that the dynamic effect on the bending of railtrack sleepers is generally high at the rail-seat and centre locations of the sleeper under 'full contact' and 'loss of contact' conditions respectively. The peak amplification factors under 'no rail-pad condition' and when the stiffness of the track structure is high. Such variations need to be adequately taken into account for the design of railtrack sleepers. Based on this study, an equivalent static model may be proposed to form a rational basis for improved design recommendations [22].

Appendix A

The equation of motion for the vehicle model comprising of carbody, bogie units and wheel sets are derived from rigid-body idealization.

Car body: The equation of motion is written for bounce (z_c), pitch (θ_c) and roll (ϕ_c) degrees of freedom with respect to transverse horizontal centroidal axis.

(a) z_c bounce of the car body

$$m_c\ddot{z}_c + 4c_p\dot{z}_c - 2c_s\dot{z}_{b1} - 2c_s\dot{z}_{b2} + 4k_pz_c - 2k_sz_{b1} - 2k_sz_{b2} = 0. \tag{A.1}$$

(b) θ_c pitch of the car body

$$J_{cy}\ddot{\theta}_c + 4c_sl_c^2\dot{\theta}_c - 2c_s\dot{z}_{b1}l_c + 2c_s\dot{z}_{b2}l_c + 4k_sl_c^2\theta_c - 2k_sz_{b1}l_c + 2k_sz_{b2}l_c = 0. \tag{A.2}$$

(c) ϕ_c roll of the car body

$$J_c\ddot{\phi}_c + 4c_s\dot{z}_cl_s + 4c_sl_s^2\dot{\phi}_c - 2c_s\dot{\phi}_{b1}l_s^2 - 2c_s\dot{\phi}_{b2}l_s^2 + 4k_sz_cl_s + 4k_sl_s^2\phi_c - 2k_s\phi_{b1}l_s^2 - 2k_s\phi_{b2}l_s^2 = 0. \tag{A.3}$$

Bogie frames: The equation of motion is written for bounce (z_b), pitch (θ_b) and roll (ϕ_b) degrees of freedom with respect to transverse horizontal centroidal axis.

(a) z_{b1} bounce of the first bogie frame

$$m_b\ddot{z}_{b1} + 2c_s\dot{z}_{b1} + 2c_s l_c\dot{\theta}_c - 2c_s\dot{z}_c + 4c_p\dot{z}_{b1} - 2c_p\dot{z}_{w1} - 2c_p\dot{z}_{w2} + 2k_s z_{b1} + 2k_s l_c\theta_c - 2k_s z_c + 4k_p z_{b1} - 2k_p z_{w1} - 2k_p z_{w2} = 0. \quad (A.4)$$

Similarly for other bogie frame z_{b2}

$$m_b\ddot{z}_{b2} + 2c_s\dot{z}_{b2} + 2c_s l_c\dot{\theta}_c - 2c_s\dot{z}_c + 4c_p\dot{z}_{b2} - 2c_p\dot{z}_{w3} - 2c_p\dot{z}_{w4} + 2k_s z_{b2} + 2k_s l_c\theta_c - 2k_s z_c + 4k_p z_{b2} - 2k_p z_{w3} - 2k_p z_{w4} = 0. \quad (A.5)$$

(b) θ_{b1} pitch of the first bogie frame

$$J_{by}\ddot{\theta}_{b1} + 4c_s l_b^2\dot{\theta}_{b1} - 2c_p\dot{z}_{w1}l_b + 2c_p\dot{z}_{w2}l_b + 4k_s l_b^2\theta_{b1} - 2k_p z_{w1}l_b + 2k_p z_{w2}l_b = 0. \quad (A.6)$$

Similarly for other bogie frame θ_{b2}

$$J_{by}\ddot{\theta}_{b2} + 4c_s l_b^2\dot{\theta}_{b2} - 2c_p\dot{z}_{w3}l_b + 2c_p\dot{z}_{w4}l_b + 4k_s l_b^2\theta_{b2} - 2k_p z_{w3}l_b + 2k_p z_{w4}l_b = 0. \quad (A.7)$$

(c) ϕ_{b1} roll of the first bogie frame

$$J_b\ddot{\phi}_{b1} + 2c_s l_s\dot{\phi}_{b1}l_s + 4c_p l_p\dot{\phi}_{b1}l_p + 2k_s l_s\phi_{b1}l_s + 4k_p l_p\phi_{b1}l_p = 0. \quad (A.8)$$

Similarly for other bogie frame ϕ_{b2}

$$J_b\ddot{\phi}_{b2} + 2c_s l_s\dot{\phi}_{b2}l_s + 4c_p l_p\dot{\phi}_{b2}l_p + 2k_s l_s\phi_{b2}l_s + 4k_p l_p\phi_{b2}l_p = 0. \quad (A.9)$$

Wheel sets: The equation of motion is written for bounce (z_w), pitch (θ_w) and roll (ϕ_w) degrees of freedom with respect to transverse horizontal centroidal axis.

(a) z_{w1} bounce of the first wheel sets

$$m_w\ddot{z}_{w1} + 2c_p\dot{z}_{w1} - 2c_p\dot{z}_{b1} + 2c_p l_b\dot{\theta}_{b1} + 2k_p z_{w1} - 2k_p z_{b1} + 2k_p l_b\theta_{b1} + 2k_w z_{w1} = R(t)_1. \quad (A.10)$$

Similarly for other wheel sets z_{w2}, z_{w3}, z_{w4}

$$m_w\ddot{z}_{w2} + 2c_p\dot{z}_{w2} - 2c_p\dot{z}_{b1} + 2c_p l_b\dot{\theta}_{b1} + 2k_p z_{w2} - 2k_p z_{b1} + 2k_p l_b\theta_{b1} + 2k_w z_{w2} = R(t)_2, \quad (A.11)$$

$$m_w\ddot{z}_{w3} + 2c_p\dot{z}_{w3} - 2c_p\dot{z}_{b2} + 2c_p l_b\dot{\theta}_{b2} + 2k_p z_{w3} - 2k_p z_{b2} + 2k_p l_b\theta_{b2} + 2k_w z_{w3} = R(t)_3, \quad (A.12)$$

$$m_w\ddot{z}_{w4} + 2c_p\dot{z}_{w4} - 2c_p\dot{z}_{b2} + 2c_p l_b\dot{\theta}_{b2} + 2k_p z_{w4} - 2k_p z_{b2} + 2k_p l_b\theta_{b2} + 2k_w z_{w4} = R(t)_4. \quad (A.13)$$

(b) ϕ_{w1} roll of the first wheel sets

$$J_{wx}\ddot{\phi}_{w1} - 2c_p l_g\dot{\phi}_{w1}l_p - 2c_p l_b\dot{\phi}_{b1}l_p + 2k_w\phi_{w1}l_g^2 - 2k_p l_g\phi_{w1}l_p - 2k_p l_b\phi_{b1}l_p = R(t)_5. \quad (A.14)$$

Similarly for other wheel sets ϕ_{w2}, ϕ_{w3}, ϕ_{w4}

$$J_{wx}\ddot{\phi}_{w2} - 2c_p l_g\dot{\phi}_{w2}l_p - 2c_p l_b\dot{\phi}_{b1}l_p + 2k_w\phi_{w2}l_g^2 - 2k_p l_g\phi_{w2}l_p - 2k_p l_b\phi_{b1}l_p = R(t)_6, \quad (A.15)$$

$$J_{wx}\ddot{\phi}_{w3} - 2c_p l_g\dot{\phi}_{w3}l_p - 2c_p l_b\dot{\phi}_{b2}l_p + 2k_w\phi_{w3}l_g^2 - 2k_p l_g\phi_{w3}l_p - 2k_p l_b\phi_{b2}l_p = R(t)_7, \quad (A.16)$$

$$J_{wx}\ddot{\phi}_{w4} - 2c_p l_g\dot{\phi}_{w4}l_p - 2c_p l_b\dot{\phi}_{b2}l_p + 2k_w\phi_{w4}l_g^2 - 2k_p l_g\phi_{w4}l_p - 2k_p l_b\phi_{b2}l_p = R(t)_8. \quad (A.17)$$

The equations of motions of the vehicle can also be written in matrix notations

$$\mathbf{m}\ddot{\mathbf{y}} + \mathbf{c}\dot{\mathbf{y}} + \mathbf{k}\mathbf{y} = \mathbf{W}(t). \quad (A.18)$$

The above equation of motion for the entire vehicle model can be written in terms of the sub-matrices as

$$\mathbf{m} = \mathrm{diag}[m_c \;\; m_{b1} \;\; m_{b2} \;\; m_{w1} \;\; m_{w2} \;\; m_{w3} \;\; m_{w4} \;\; I_c \;\; I_{b1} \;\; I_{b2} \;\; J_c \;\; J_{b1} \;\; J_{b1} \;\; J_{w1} \;\; J_{w2} \;\; J_{w3} \;\; J_{w4}],$$

where $\mathbf{m}$ is the mass matrix written in diagonal form,
$\ddot{\mathbf{y}}^{\mathrm{T}}$ is the acceleration vector,

$$\ddot{\mathbf{y}}^{\mathrm{T}} = \{\, \ddot{z}_c \quad \ddot{z}_{b1} \quad \ddot{z}_{b2} \quad \ddot{z}_{w1} \quad \ddot{z}_{w2} \quad \ddot{z}_{w3} \quad \ddot{z}_{w4} \quad \ddot{\theta}_c \quad \ddot{\theta}_{b1} \quad \ddot{\theta}_{b2} \quad \ddot{\phi}_c \quad \ddot{\phi}_{b1} \quad \ddot{\phi}_{b2} \quad \ddot{\phi}_{w1} \quad \ddot{\phi}_{w2} \quad \ddot{\phi}_{w3} \quad \ddot{\phi}_{w4} \,\},$$

$[\mathbf{c}]^1$ and $[\mathbf{c}]^2$ are the sub-matrices of the damping matrix

$$[\mathbf{c}]^1 = \begin{bmatrix}
4c_s & -2c_s & -2c_s & 0 & 0 & 0 & 0 & 0 & 0 & 0 \\
-2c_s & 2c_s + 2c_p & 0 & -2c_p & -2c_p & 0 & 0 & 2c_s l_c & 0 & 0 \\
-2c_s & 0 & 2c_s + 2c_p & 0 & 0 & -2c_p & -2c_p & -2c_s l_c & 0 & 0 \\
0 & -2c_p & 0 & 2c_p & 0 & 0 & 0 & 0 & 2c_p l_b & 0 \\
0 & -2c_p & 0 & 0 & 2c_p & 0 & 0 & 0 & -2c_p l_b & 0 \\
0 & 0 & -2c_p & 0 & 0 & 2c_p & 0 & 0 & 0 & 2c_p l_b \\
0 & 0 & -2c_p & 0 & 0 & 0 & 2c_p & 0 & 0 & -2c_p l_b \\
0 & 2c_s l_c & -2c_s l_c & 0 & 0 & 0 & 0 & 2c_s l_c^2 & 0 & 0 \\
0 & 0 & 0 & 2c_p l_b & -2c_p l_b & 0 & 0 & 0 & 2c_p l_b^2 & 0 \\
0 & 0 & 0 & 0 & 0 & 2c_p l_b & -2c_p l_b & 0 & 0 & 2c_p l_b^2
\end{bmatrix},$$

$$[\mathbf{c}]^2 = \begin{bmatrix}
4c_s l_{c1}^2 & -2c_s l_{c1}^2 & -2c_s l_{c1}^2 & 0 & 0 & 0 & 0 \\
-2c_s l_{c1}^2 & \begin{matrix}2c_s l_{c1}^2 \\ +4c_p l_{b1}^2\end{matrix} & 0 & -2c_p l_{b1} l_g & -2c_p l_{b1} l_g & 0 & 0 \\
-2c_s l_{c1}^2 & 0 & \begin{matrix}2c_s l_{c1}^2 \\ +2c_p l_{b1}^2\end{matrix} & 0 & 0 & -2c_p l_{b1} l_g & -2c_p l_{b1} l_g \\
0 & -2c_p l_{b1}^2 & 0 & 2c_p l_{b1} l_g & 0 & 0 & 0 \\
0 & -2c_p l_{b1}^2 & 0 & 0 & 2c_p l_{b1} l_g & 0 & 0 \\
0 & 0 & -2c_p l_{b1}^2 & 0 & 0 & 2c_p l_{b1} l_g & 0 \\
0 & 0 & -2c_p l_{b1}^2 & 0 & 0 & 0 & 2c_p l_{b1} l_g
\end{bmatrix},$$

$\{\dot{\mathbf{y}}_1\}^{\mathrm{T}}$ and $\{\dot{\mathbf{y}}_2\}^{\mathrm{T}}$ are the velocity vectors,

$$\{\dot{\mathbf{y}}_1\}^{\mathrm{T}} = \{\, \dot{\mathbf{z}}_c \quad \dot{\mathbf{z}}_{b1} \quad \dot{\mathbf{z}}_{b2} \quad \dot{\mathbf{z}}_{w1} \quad \dot{\mathbf{z}}_{w2} \quad \dot{\mathbf{z}}_{w3} \quad \dot{\mathbf{z}}_{w4} \quad \dot{\theta}_c \quad \dot{\theta}_{b1} \quad \dot{\theta}_{b2} \,\},$$
$$\{\dot{\mathbf{y}}_2\}^{\mathrm{T}} = \{\, \dot{\phi}_c \quad \dot{\phi}_{b1} \quad \dot{\phi}_{b1} \quad \dot{\phi}_{w1} \quad \dot{\phi}_{w2} \quad \dot{\phi}_{w3} \quad \dot{\phi}_{w4} \,\},$$

$[\mathbf{k}]^1$ and $[\mathbf{k}]^2$ are the sub-matrices of the stiffness matrix

$$[\mathbf{k}]^1 = \begin{bmatrix} 4k_s & -2k_s & -2k_s & 0 & 0 & 0 & 0 & 0 & 0 & 0 \\ -2k_s & 2k_s+2k_p & 0 & -2k_p & -2k_p & 0 & 0 & 2k_s l_c & 0 & 0 \\ -2k_s & 0 & 2k_s+4k_p & 0 & 0 & -2k_p & -2k_p & -2k_s l_c & 0 & 0 \\ 0 & -2k_p & 0 & 2k_p & 0 & 0 & 0 & 0 & 2k_p l_b & 0 \\ 0 & -2k_p & 0 & 0 & 2k_p & 0 & 0 & 0 & -2k_p l_b & 0 \\ 0 & 0 & -2k_p & 0 & 0 & 2k_p & 0 & 0 & 0 & 2k_p l_b \\ 0 & 0 & -2k_p & 0 & 0 & 0 & 2k_p & 0 & 0 & -2k_p l_b \\ 0 & 2k_s l_c & -2k_s l_c & 0 & 0 & 0 & 0 & 4k_s l_c^2 & 0 & 0 \\ 0 & 0 & 0 & 2k_p l_b & -2k_p l_b & 0 & 0 & 0 & 4k_p l_b^2 & 0 \\ 0 & 0 & 0 & 0 & 0 & 2k_p l_b & -2k_p l_b & 0 & 0 & 4k_p l_b^2 \end{bmatrix},$$

$$[\mathbf{k}]^2 = \begin{bmatrix} 4k_s l_{c1}^2 & -2k_s l_{c1}^2 & -2k_s l_{c1}^2 & 0 & 0 & 0 & 0 \\ -2k_s l_{c1}^2 & 2k_s l_{c1}^2 + 4k_p l_{b1}^2 & 0 & -2k_p l_{b1} l_g & -2k_p l_{b1} l_g & 0 & 0 \\ -2k_s l_{c1}^2 & 0 & 4k_s l_{c1}^2 + 2k_p l_{b1}^2 & 0 & 0 & -2k_p l_{b1} l_g & -2k_p l_{b1} l_g \\ 0 & -2k_p l_{b1}^2 & 0 & 2k_p l_{b1} l_g & 0 & 0 & 0 \\ 0 & -2k_p l_{b1}^2 & 0 & 0 & 2k_p l_{b1} l_g & 0 & 0 \\ 0 & 0 & -2k_p l_{b1}^2 & 0 & 0 & 2k_p l_{b1} l_g & 0 \\ 0 & 0 & -2k_p l_{b1}^2 & 0 & 0 & 0 & 2k_p l_{b1} l_g \end{bmatrix},$$

$\{\mathbf{y}_1\}^{\mathrm{T}}$ and $\{\mathbf{y}_2\}^{\mathrm{T}}$ are the displacement vectors

$$\{\mathbf{y}_1\}^{\mathrm{T}} = \{ z_c \quad z_{b1} \quad z_{b2} \quad z_{w1} \quad z_{w2} \quad z_{w3} \quad z_{w4} \quad \theta_c \quad \theta_{b1} \quad \theta_{b2} \},$$

$$\{\mathbf{y}_2\}^{\mathrm{T}} = \{ \phi_c \quad \phi_{b1} \quad \phi_{b1} \quad \phi_{w1} \quad \phi_{w2} \quad \phi_{w3} \quad \phi_{w4} \},$$

$$\mathbf{W}(t)^{\mathrm{T}} = \{0\ 0\ 0\ R(t)_1\ R(t)_2\ R(t)_3\ R(t)_4\ 0\ 0\ 0\ 0\ 0\ 0\ R(t)_5\ R(t)_6\ R(t)_7\ R(t)_8\},$$

where $\mathbf{m}$, $\mathbf{c}$ and $\mathbf{k}$ are the mass, damping and stiffness matrices of the vehicle, respectively, and $\mathbf{W}(t)$ is load vector, and $R(t)_j$ denotes the reactive force (corresponding to the jth degree of freedom) obtained by algebraic summation of reactions from the two rails.

References

[1] A.N. Talbot, Stresses in Railroad Track—Reports of the Special Committee on Stresses in Railroad Track, Seventh Progress Report, American Railway Engineering and Maintenance of Way Association, AREMA, 1934.

[2] A.N. Hanna, State of the art report on prestressed concrete ties for North American railroads, Portland Cement Association Research Journal 5 (1979) 31–61.

[3] H.P.J. Taylor, The prestressed concrete railway sleepers—50 years of pretensioned, prestressed concrete, The Structural Engineer 71 (1993) 281–289.
[4] G.C. Agarwal, P.G. Agwekar, Use of high strength concrete for prestressed concrete sleepers in India, Indian Concrete Journal 6 (1996) 683–686.
[5] Standard Specification for Pretensioned Concrete Sleepers, RDSO Third Revision, Indian Railways, India, 1996.
[6] S.L. Grassie, S.J. Cox, The dynamic response of railway track with flexible sleepers to high frequency vertical excitation, Proceedings of the Institution of Mechanical Engineers 198-D (1983) 117–124.
[7] K.L. Knothe, S.L. Grassie, Railway track and vehicle/track interaction, Journal of Vehicles System Dynamics 22 (1993) 217–262.
[8] J.C.O. Nielsen, Vertical dynamic interaction between train and track—influence of wheel and track imperfections, Journal of Sound and Vibration 87 (5) (1995) 825–839.
[9] J. Oscarsson, T. Dahlberg, Dynamic train/track interaction—computer models and full scale experiments, Journal of Vehicle System Dynamics 29 (1998) 73–84.
[10] B. Ripke, K. Knothe, Simulation of high frequency vehicle–track interactions, Journal of Vehicle System Dynamics Supplement 24 (1995) 72–85.
[11] G. Kumaran, D. Menon, K.K. Nair, Dynamic response of railtrack sleepers to moving train loads, Proceedings of EURODYN-02, Swets & Zeitlinger, Lisse, 2002, pp. 1185–1190.
[12] K.V. Gangadharan, Analytical and Experimental Studies on Dynamics of Railroad Vehicles, Ph.D. Thesis, Department of Applied Mechanics, Indian Institute of Technology, Madras, India, 2001.
[13] V. Dukkipati, J.R. Amyot, Computer-Aided Simulation in Railway Dynamics, Marcel Dekker, New York, 1988.
[14] A.G. Kerr, Proceedings of a Symposium on Railroad Track Mechanics and Technology, Pergamon Press, Princeton, 1985.
[15] K.J. Bathe, E.L. Wilson, Numerical Methods in Finite Element Analysis, Prentice-Hall, Englewood Cliffs, NJ, 1976.
[16] C.S. Desai, A.M. Siriwardane, Numerical models for track support structures, Journal of Geotechnical Engineering Division, American Society of Chemical Engineers 108 (1982) 461–480.
[17] J. Dinkel, H. Grundmann, Winkler parameters for railway dynamics derived from 3-D half space analysis, Proceedings of EURODYN-99, 1999, pp. 831–836.
[18] D. Li, T. Ernest, Wheel/track dynamic interaction—track substructure perspective, Journal of Vehicle System Dynamics 24 (1995) 183–196.
[19] J.P. Wolf, Foundation Vibration Analysis Using Simple Physical Models, Prentice-Hall, Englewood Cliffs, NJ, 1994.
[20] A.K. Chopra, Dynamics of Structures: Theory and Applications to Earthquake Engineering, Prentice-Hall, Englewood Cliffs, NJ, 2001.
[21] G. Kumaran, D. Menon, K.K. Nair, Estimation of dynamic loading on railtrack sleepers, Proceedings of the 2nd International Conference on Wind and Structures, Basan, Korea, 21–23 August, 2002, pp. 127–134.
[22] G. Kumaran, Formulation of Improved Design Basis for Prestressed Concrete Railtrack Sleepers, Ph.D. Thesis, Dept. of Civil Engineering, IIT Madras, 2002.
[23] G. Kumaran, D. Menon, K.K. Nair, Evaluation of dynamic load on railtrack sleepers based on vehicle-track modeling and analysis, International Journal of Structural Stability and Dynamics 2 (3) (2002) 355–374.